Landscape Ecology **16:** 471–490, 2001.

Research Article

A multiscale framework for landscape analysis: Object-specific analysis and upscaling

G.J. Hay[1,*], D.J. Marceau[1], P. Dubé[1] and A. Bouchard[2]
[1]*Geocomputing Laboratory, Département de géographie, Université de Montréal, C.P. 6128, succursale Centre-Ville, Montréal, Qué, Canada, H3C 3J7;* [2]*IRBV, Université de Montréal, Jardin Botanique de Montréal, 4101 Sherbrooke Est, Montréal, Qué, Canada. H1X2B2;* [*]*Author for correspondence (Tel: (514) 343-8073; Fax: (514) 343-8008; E-mail: ghay@sympatico.ca)*

Received 15 October 1999; Revised 10 April 2001; Accepted 5 April 2001

Key words: domains of scale, image-objects, landscape thresholds, MAUP, multiscale, object-specific analysis, OSA, OSU, remote sensing, scale, upscaling

Abstract

Landscapes are complex systems that require a multiscale approach to fully understand, manage, and predict their behavior. Remote sensing technologies represent the primary data source for landscape analysis, but suffer from the modifiable areal unit problem (MAUP). To reduce the effects of MAUP when using remote sensing data for multiscale analysis we present a novel analytical and upscaling framework based on the spatial influence of the dominant objects composing a scene. By considering landscapes as hierarchical in nature, we theorize how a multiscale extension of this object-specific framework may assist in automatically defining critical landscape thresholds, domains of scale, ecotone boundaries, and the grain and extent at which scale-dependent ecological models could be developed and applied through scale.

Introduction

To better understand, manage, and predict the behavior of the complex systems that provide life on earth, we require an improved understanding of the scale-specific interactions responsible for landscape metabolism (Levin 1992), robust techniques for visualizing and deciphering multiscale processes from patterns (Turner et al. 1991), and appropriate scaling strategies for linking and modelling data at multiple scales (King 1990; Ehleringer and Field 1993). To assist landscape ecologists in these tasks modern remote sensing technologies provide multi-resolution data sources for analysis and hypothesis testing over both large and small areas, and hierarchy theory provides a useful analytical framework for describing the landscape's composition within these scenes.

According to hierarchy theory, ecological systems are considered as 'nearly decomposable' hierarchically organized entities resulting from (different) structuring processes exerting their influence over defined ranges or domains of scale (Allen and Starr 1982; O'Neill et al. 1986; Holling 1992). Conceptually, the decomposability of these systems implies that their analysis and understanding can be enhanced by organizing their numerous components into fewer discrete, interactive units at different levels based on differences in process rates (O'Neill et al. 1989; King 1999). When these ideas are considered in relation to the spatial, spectral, temporal, and radiometric properties inherent to remote sensing data (Marceau and Hay 1999a), the keys to fully unlock the complex relationships between scale-specific landscape patterns and processes appear close at hand. For example, Moody and Woodcock (1995), Benson and MacKenzie (1995), O'Neill et al. (1996), and Pax-Lenney and Woodcock (1997) describe the influence of remote sensing resolution on detecting landscape patterns and processes. Bian and Walsh (1993), Souriau (1994) and Walsh et al. (1997) discuss the identification of

Table 1. List of general terms and abbreviations.

AVHRR	Advanced very high resolution radiometer
AVIRIS	Airborne Visible Infra-Red Imaging Spectrometer
C.Cut	Clear-cut
CASI	Compact Airborne Spectrographic Imager
CCD	Charged-couple device
DNs	Digital numbers or gray-scale values
FPAR	Fraction of photosynthetically active radiation
HPDP	Hierarchical Patch Dynamics Paradigm
H-res	High resolution
IFOV	Instantaneous field of view
LAI	Leaf area index
L-res	Low resolution
MAUP	Modifiable areal unit problem
MODIS	Moderate-resolution Imaging Spectroradiometer
PSF	Point-spread function
RMSE	Root mean square error
SPOT	Satellite pour l'Observation de la Terre
TM	Landsat Thematic Mapper

landscape scale-thresholds and domains of scale as viewed in remotely sensed data. Caldwell et al. (1993), Ustin et al. (1993), Friedl et al. (1995), Cullinan et al. (1997), DeFries et al. (1997), and Stewart et al. (1998) describe the challenges of scaling remote sensing data and the implementation of multiscale approaches for ecosystem models.

In addition to the remote sensing platforms more familiar to landscape ecologists such as AVHRR$^{\otimes}$, TM$^{\otimes}$ and SPOT$^{\otimes}$, lesser-known hyperspectral airborne sensors like CASI$^{\otimes}$ and AVIRIS$^{\otimes}$ have been in operation for over a decade providing unique opportunities to diagnostically examine landscape patterns and processes at very fine spatial and spectral scales (Wessman et al. 1989). These sensors allow for the discrimination of landscape structures that are absent in coarser imagery, thus providing opportunities to link field data with patterns at much coarser scales (Treitz and Howarth 2000). They also serve as excellent test-beds for conducting fine-scale landscape analysis in preparation for data available from the new high-resolution satellites such as Ikonos (with its commercially available 1 m^2 panchromatic and 4 m^2 multispectral channels), MODIS$^{\otimes}$ (with its 36 co-registered channels ranging from 250 m^2–1 km^2), and Hyperion (launched in November, 2000 with a capacity to acquire 220 spectral bands (from 0.4 to 2.5 μm) at a 30 m^2 spatial resolution).

$^{\otimes}$See Table 1.

It is becoming increasingly apparent that in order to fully understand the complexity of landscape dynamics we require the ability to recognize broad-scale patterns and processes, and relate them to those at finer scales where we are most familiar (Wu and Qi 2000). These high-resolution sensors provide critical data and perspectives that will assist in bridging this knowledge gap.

While remote sensing data hold great promise, it is also important to recognize their limitations. In particular, all remote sensing data represent a unique form of the *modifiable unit areal problem* or the MAUP (for a comprehensive review see Marceau 1999). Though the importance of MAUP has previously been noted in landscape ecology (Jelinski and Wu 1996), its relationship to remote sensing data remains poorly recognized and understood (Wu et al. 2000). In particular, the effects of MAUP can be especially devastating during scaling, where arbitrarily extrapolating site-specific measurements to coarser scales can result in substantial error (Gardner et al. 1982; King 1990). Thus the ramifications for inappropriately using remote sensing data to understand multiscale landscape patterns/processes are profound. This is especially relevant in landscape ecology, where multiscale studies are increasingly conducted (Wu and Qi 2000), and where land-cover classifications generated from satellite imagery are frequently used to characterize the ecology of large areas and to make generalizations about the distribution of species and communities (Townsend 2000).

The primary objectives of this paper are to describe a novel approach for analyzing and upscaling remotely sensed data, and a multiscale extension to this approach, both of which are based on the spatial influence of the dominant objects composing the scene, rather than relying solely on user bias. These novel approaches incorporate object-specific analysis and solutions to the MAUP. Together they represent a framework for spatially defining critical landscape thresholds and domains of scale, ecotone boundaries, and the grain and extent at which scale-dependent ecological models could be developed, and applied.

Theoretical background

The following two sections briefly provide a theoretical background on scale, scaling, the relationship between remote sensing imagery and MAUP, and the

fundamentals of object-specific analysis and object-specific upscaling, and their relationship with other scaling techniques.

Scale, scaling, remote sensing imagery and MAUP

Conceptually, scale represents the 'window of perception', the filter, or measuring tool with which a system is viewed and quantified. As scale changes, so do the associated patterns of reality, which has obvious implications for understanding any organism, place, or system. An important characteristic of scale lies in the distinction between grain and extent. *Grain* refers to the smallest intervals in an observation set, while *extent* refers to the range over which observations at a particular grain are made (O'Neill and King 1998). Within a remote sensing context, grain is equivalent to the spatial resolution of the pixels composing an image, while extent represents the total area that an image covers.

Associated with multiscale analysis is the term *domain of scale* (or scale domain). This refers to a region of the scale spectrum over which, for a particular phenomenon, patterns do not change or change monotonically with changes in scale. Such domains are separated by *scale thresholds* - relatively sharp transitions or critical points along the spatial scale continuum where a shift in the relative importance of variables influencing a process occur (Meentemeyer 1989; Wiens 1989).

To analyze objects, or entire scenes at different scales, and to utilize information between these scales, appropriate *scaling* methods are required. Scaling refers to transferring data or information from one scale to another. It requires the identification of the factors operational at a given scale of observation, their congruency with those on the lower and higher scales, and the constraints and feedbacks on those factors (Caldwell et al. 1993). As noted by Jarvis (1995), scaling represents a real challenge because of the non-linearity between processes and variables, and heterogeneity in properties that determines the rates of processes. In practice, scaling can be performed from a 'bottom-up' or a 'top-down' approach: *upscaling* consists of using information at smaller scales to derive information at larger scales, while *downscaling* consists of decomposing information at one scale into its constituents at smaller scales.

Allen and Hoekstra (1991) suggest that scale is not a property of nature alone but rather is something associated with observation and analysis, and that the scale of a process is fixed only once the observer has specified the actors in the system. So what happens when the scale of observation is arbitrarily derived, as is the case with remote sensing data? Quantification problems resulting from such arbitrariness are known as the *modifiable unit areal problem* or the MAUP (Openshaw and Taylor 1979; Openshaw 1981).

The MAUP originates from the fact that a significant number of different – often arbitrary – ways exist by which a study area can be divided into non-overlapping areal units for the purpose of spatial analysis. In essence, the MAUP represents the sensitivity of analytical results to the definition of data collection units, and is illustrated by two related but distinct components: the *scale problem* and the *aggregation problem*. The former is the variation in results that can be obtained when areal units are progressively aggregated into fewer, larger units for analysis; the latter represents the variation in results generated by the use of alternative aggregation schemes at equal or similar resolutions (Openshaw 1984). Consequently, the potential for error in the analysis of spatial data resulting from MAUP is significant, and has been recognized in a number of studies (Dudley 1991; Fotheringham and Wong 1991; Hunt and Boots 1996).

Marceau (1992) was among the first to demonstrate that remote sensing data represent a particular case of the MAUP. In a remote sensing scene, an image may be envisioned as a regular net arbitrarily thrown over a study area where the grain and extent of the mesh define the areal units measured (Figure 1). More correctly, each pixel represents an integrated radiance measure corresponding to the spectral, spatial, temporal, and radiometric influence of the real-world objects within the area delineated by the instantaneous field of view (IFOV) of the sensor (Duggin and Robinove 1990). IFOV determines how much of the ground area the sensor 'sees' at any given instant in time. This results in three general situations: the ground features of interest are smaller than, approximately equal to, or larger than the spatial sampling unit. It should be noted that within a single image, each of these sampling combinations are possible, and in fact very probable. In the first situation, this type of image is referred to as *low resolution* or *L-res*, in the second and third cases, as *high resolution* or *H-res* (Woodcock and Strahler 1987). Consequently, every image is characterized by a scale and aggregation level, which determines its structure and information content. Recognizing this is critical for determining what information can be ex-

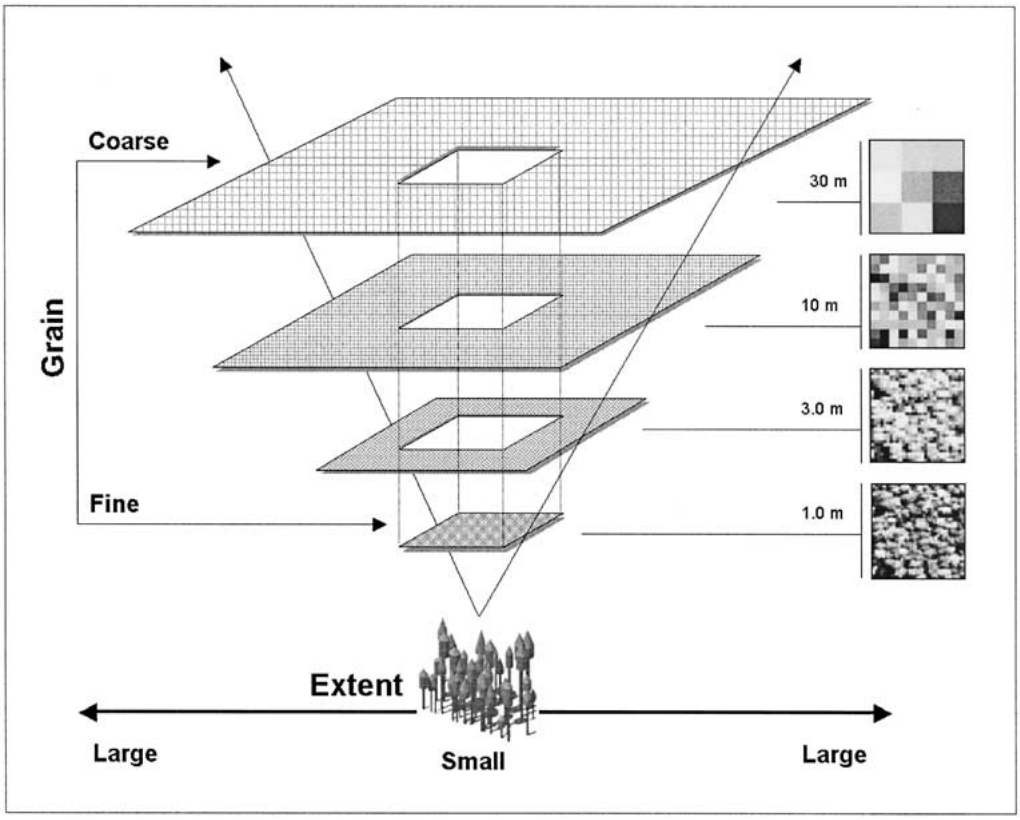

Figure 1. The relationship between grain and extent in remote sensing imagery.

tracted from an image, and how reliable it is (Marceau et al. 1994).

Fortunately, several solutions to MAUP have been suggested (Fotheringham 1989). In particular we note two important concepts related to these solutions. First, the MAUP does not exist if analysis is performed with basic entities. The term *basic entity* refers to an object composed of similar parts that are different than itself. For example, if we consider a tree-crown as a basic entity, conceptually it may be *composed of*, or is an *aggregate of* leaves, and branches, each of which individually belongs to classes that are themselves, basic entities. Thus, identifying basic entities provides the clearest way out of the MAUP, as a user works with spatially discrete entities rather than arbitrarily defined areal units (for additional information see Fotheringham, 1989). Second, while the MAUP certainly poses significant challenges, it can also reveal critical information for understanding the structure, function, and dynamics of complex real world systems if it is recognized and dealt with explicitly (Jelinski and Wu 1996). Part of the challenge in recognizing MAUP is that there is no unique 'MAUP statistic' to quantify its influence, though correlation analysis and other techniques have been used (Amrhein and Reynolds 1996; Hunt and Boots 1996). Instead, users of spatial data must be cognizant of the fact that spatial analysis of arbitrarily defined areal units can produce results that may not necessarily represent the content of the original units, but rather, the associations between them (i.e., aggregation problem) and the scale at which they were assessed (i.e., scale problem).

The fundamentals of Object-Specific Analysis (OSA) and Upscaling (OSU)

Object-Specific Analysis (OSA) is a multiscale technique that defines unique spatial measures, specific to the individual objects composing a remote sensing scene. These object-specific measures are then used in weighting functions for upscaling an image to a coarser resolution. The resolution of the upscaled image can either be defined manually by the user (see further), or automatically by statistical properties of the objects composing the image (see further).

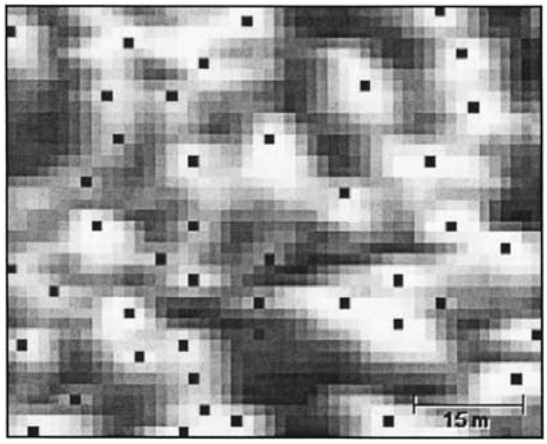

Figure 2. Tree-crown image-objects. This CASI sub-image has been magnified to illustrate the relationship between individual pixels (gray-tone squares) and the tree-crown image-objects they perceptually represent. Individual crown centers are defined by a single black pixel. The spatial resolution of each pixel is 1.5 m^2.

Both forms of upscaling are referred to as Object-Specific Upscaling (OSU) because they incorporate object-specific weights. Thus, MAUP effects are minimized in both OSA and OSU, as object-specific spatial information is incorporated throughout the analysis.

An underlying premise of OSU is that H-res *image-objects* should have more influence on an upscaled signal than a single L-res pixel – which signal is already regularized[1] . The term 'image-objects' refers to basic entities, located within an image that are perceptually generated from H-res pixel groups, where each pixel group is composed of similar digital values, and possesses an intrinsic size, shape, and geographic relationship with the real-world scene component it models [e.g., a tree crown (Figure 2)].

The heuristics determining this threshold of 'similarity' are based on the novel concept that all pixels within an image are explicitly considered H-res samples of the scene-objects they model, even though (as previously described) each pixel many represent both H- and L-res object information. The importance of this rule is that by biasing for H-res samples only, we explicitly seek objects that exist at, or over, a larger spatial extent than the area covered by the individual pixels that compose them. Essentially, we are using parts of objects (grain) to define the extent of objects that exist at their next (coarser) scales. The spatial extents defined are then used as weights to representatively upscale the image to a coarser resolution.

Similar to Mandelbrot's famous question concerning the length of a coastline, the answer is dependent on the precision of the measuring tool (Mandelbrot 1967). In the case of OSA, the maximum sized object that can be defined is represented by the relationship between the spatial resolution of pixels composing the objects within a scene, and the ability of the heuristics to define this object's edges. As a result, this technique can be applied to any type of remote sensing data from H-res data such as the CASI (airborne), and Ikonos (satellite), to medium resolution TM and low-resolution AVHRR. The only difference in each case is to appreciate the relationship between the pixel size, and the geographic size of the object of which the pixel is a component. In a CASI data set, pixels could be considered parts of individual trees, trees being the object of analysis. In TM data, individual pixels may be considered parts of a particular forest stand, and in AVHRR data, individual pixels may represent parts of a larger extent, more general landscape entity such as a deciduous broad-leaf forest class.

Though sharing similarities with other scaling and scale detecting techniques (Turner et al. 1991; Gardner 1998), OSA is unique, in that it incorporates an explicit multi-resolution (i.e., hierarchical) sampling and evaluation of each pixel in relation to the (different sized) coarser grain objects of which it is a nested constituent. For example, while *scale variance analysis* (Moellering and Tobler 1972) is also a hierarchical approach, there is no consideration of pixels as parts of individual objects composing a scene. Instead, pixels composing the image are aggregated by systematically increasing grain size (for the entire image), resulting in a nested hierarchy of images with the same extent, but with different spatial resolutions. A measure of the total scene variance is then evaluated for each image in the hierarchy, and the results are plotted illustrating potential scale thresholds at specific resolutions within the entire scene. A similar approach is described by Woodcock and Strahler (1987), where local scene variance is graphed as a function of increasing spatial resolution, and also by Marceau et al. (1994) where a minimum spectral variance threshold is used to define the optimal spatial resolution of different forest classes.

In OSA, a ubiquitous 'optimal' resolution is never found, as none exists in images representing complex heterogeneous environments (Hay et al. 1997).

[1] *Regularization* is a signal-processing term describing the integration of signals generated by objects that are no longer individually discernable (thus L-res), due to the physical limitations of the sensing device in relation to the size of the objects being assessed.

Instead, different 'optimal' resolutions or thresholds are defined based on the different objects being assessed (Hay et al. 1996). In the previous examples, the described techniques are used for scale exploration only. They do not explicitly consider individual pixels as parts of variously sized, shaped, and spatially distributed objects, and they do not include facility for upscaling, or provide information indicating where in the image such spatial thresholds exist. OSA does not share these limitations.

Materials and methods

Study site

Our initial interest in scale issues was based on understanding the spatial evolution of individual trees and forest gaps through scale (Marceau and Hay 1999b), particularly as it relates to changes in landscape fragmentation. To facilitate this we applied OSA and OSU to H-res CASI data, which allowed us to follow the evolution of familiar image/site structures through scale. The CASI (Compact Airborne Spectrographic Imager) is a pushbroom sensor designed to operate from light aircraft and helicopters, with data capture capabilities based on a two-dimensional frame transfer CCD array. 16 bit signed data were collected during 20:10–21:40 h (GMT) over the Sooke Watershed, Vancouver Island, British Columbia, Canada on August 1, 1993 (Figure 3). The data were radiometrically corrected to 1.5 m^2 pixels, and a study site (Figure 4a) was located along Rithet Creek and extracted from a channel centered at 0.66 μm ($+/-$ 0.05 μm). This scene was then corrected for geometry and atmosphere, and all subsequent analyses were performed on it. Ancillary data include 1:10,000 forest inventory maps, numerous field surveys, and 1:12,000 color near-infrared (NIR) aerial photography (1993). In this area, the very dry maritime Coastal Western Hemlock biogeoclimatic subzone dominates, though a small component of moist maritime Coastal Douglas-Fir subzone also exists.

In Figure 4a, three principal stand types are visible, each of which illustrates the dominant seral tree species - Coastal Douglas-Fir [(*Pseudotsuga menziesii*) (Mirb.) Franco var. *menziesii*]. Located in the center of this image is a mature stand (141–250 yrs) with a crown-closure of 56–65%. Below it (bottom center) is a dense young stand (21–30 yrs) with a crown-closure of 76–85%. Surrounding these two, notably on the image left, is a stand of mixed-immature and mixed-young individuals (1–20 yrs), with crown closures ranging from 0–45%. Three gravel roads transect the scene and are represented as bright linear features. An exposed sparsely vegetated clear-cut (C.Cut) lies adjacent to a gravel road at the upper right quadrant of the scene, and a small, partially vegetated marsh is located at the bottom right. Throughout the site, many exposed soil, and soil-grass patches are visible. In the Thematic Map (Figure 4b), these patches have been classified as C.Cut.

OSA and user-defined OSU

In the earth sciences it is generally observed that objects closer to each other are more alike than those further apart (Curran and Atkinson 1998). Similarly, in a remotely sensed image, spatially near pixels tend to elicit a strong degree of spectral autocorrelation. Therefore, plotting the digital variance of samples (pixels) located within increasingly larger kernels, while centered on an image-object of known size tends to produce a distinct break, or threshold in variance as increasing sized kernels contact the image-object's edges. The unique window size (VT_w) defined at this variance threshold location (VT_{ij}) corresponds explicitly to the object's known size, and is a key component for determining object-specific weighting values [i and j represent row and column within the original CASI image (O_I)]. Conceptually, VT_w may be considered similar to *lag* as described when using semivariance. For example, the window size at location (A) in Figure 5 represents the maximum scale for defining the (inset) tree-crown[2]. Locations B-C, D-E, and F-G, represent an object-specific range of 'optimal' window sizes for defining the nested image-objects, of which the center tree-crown pixel (white dot) is a member. Locations B, D, and F represent the local variance minima corresponding to the scales where the next set of 'nested' objects are first manifest. Minimum variance indicates that the pixels composing this measure are locally the most spectrally similar, thus they are the most 'object-like', while variance maxima located at C, E, and G, respectively, represent the maximum spatial extents of these nested objects. Locations A-B, C-D, and E-F are explained in the Discussion section.

The window size at one iteration prior to VT_{ij} is used to define the maximum area (A_{ij}) at which the

[2]The inset image has been extracted form the mature-stand in O_I, and the corresponding curve represents the actual variance values determined at each incremented widow size.

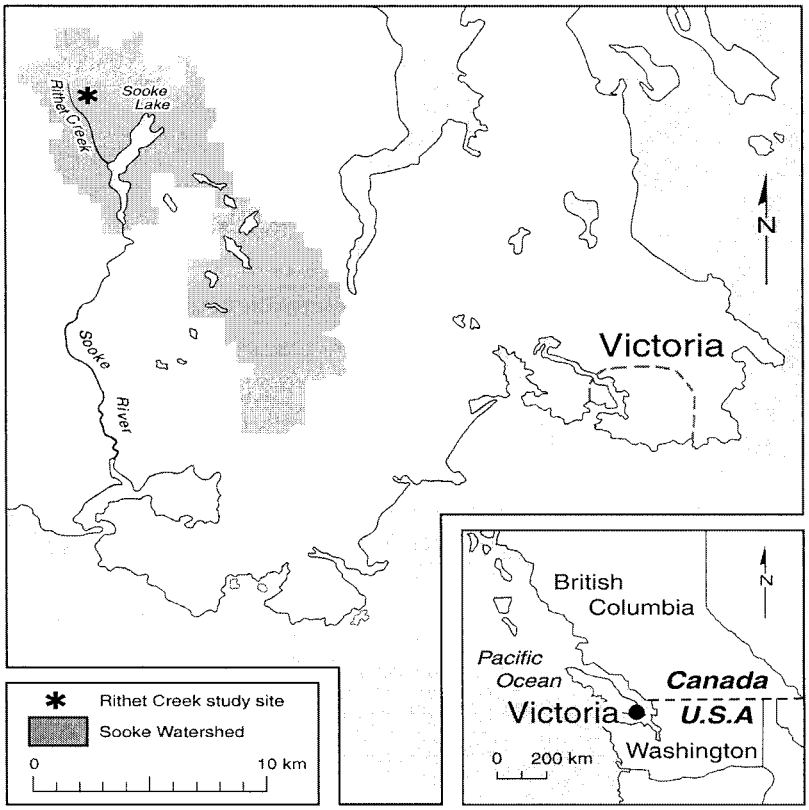

Figure 3. Rithet Creek study site map.

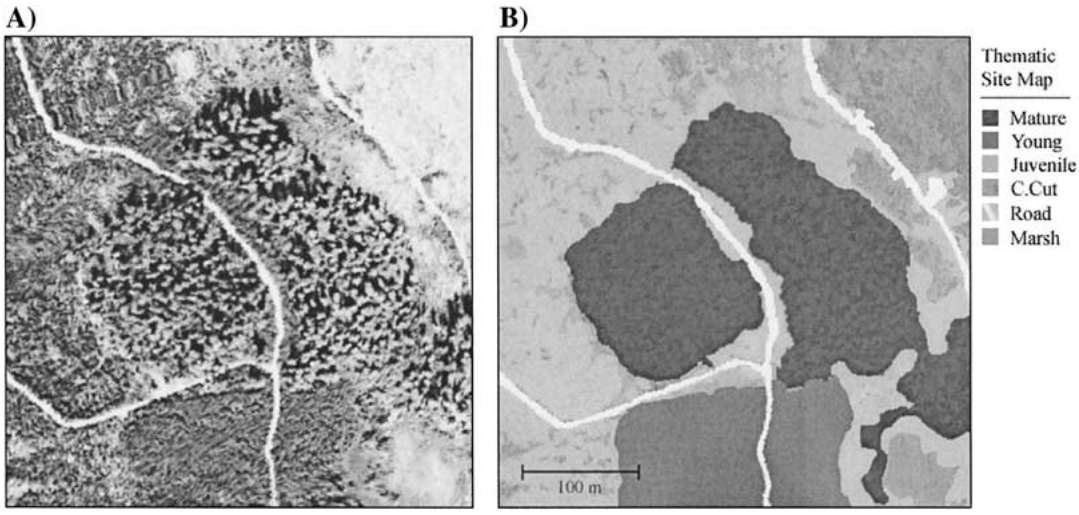

Figure 4. Remote sensing image and thematic map of the study site. A). CASI image illustrating the study area (36 ha^2) at a spatial resolution of 1.5 m^2. B). Thematic site map and legend (same scale).

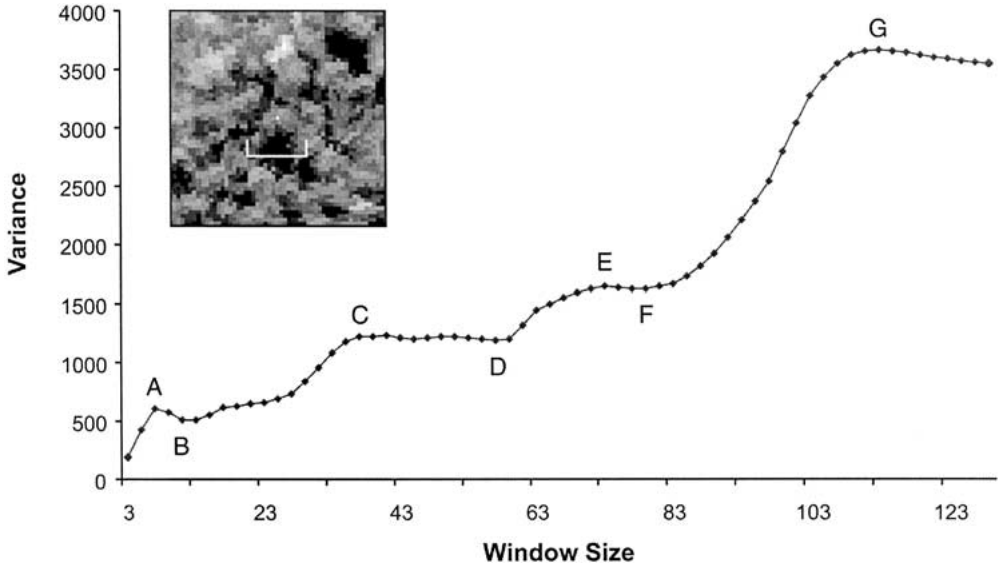

Figure 5. Variance characteristics of a single tree-crown pixel defined through multiple scales. The curve of this graph results from plotting the variance of the digital values of all pixels located within increasing sized square windows. In this illustration, varying sized windows are centered over an individual tree-crown (circular image-object) that is located within the white bars of the inset image. The crown center is defined by a single white pixel that represents the apex of the tree. As the window size increases, the resulting variance value is plotted. In practice this form of multiscale analysis is applied to all pixels composing a scene. The maximum window size specified for each pixel is defined when variance measures meet unique object-specific heuristics that correspond to the spatial extent of the real-world objects they model.

central pixel under analysis is spectrally and spatially related to its neighbours. At the same time that A_{ij} is defined, the corresponding mean (M_{ij}) and variance (V_{ij}) values are also defined for the central pixel within VT_w. These procedures are then applied to all remaining pixels in O_I, resulting in corresponding variance (V_I), area (A_I), and mean (M_I) images.

Once V_I, A_I, and M_I have been generated, two steps are required to complete user-defined OSU. The first involves determining an object-specific weight (W_{ij}) for each ($\forall$) pixel (P_{ij}) in O_I, which is represented by W_{ijK}.

$$\forall P_{ij} \in O_I \tag{1}$$

$$W_{ijK} = (A_{ijK}/S_K)$$

W_{ijK} defines the object-specific weight for each A_{ij} within an upscaling kernel (K) [of a (k*k) user-defined dimension], where S_K is the sum of all A_{ij} within K (see equation 2).

$$S_K = \sum_{i}^{k} \sum_{j}^{k} A_{ij} \tag{2}$$

The second step is to apply the object-specific weight to produce a new upscaled image.

$$\forall UP_{LM} \in U_I$$

$$UP_{LM} = \left[\sum_{L}^{k} \sum_{M}^{k} (O_{ij} {}^{*} W_{ij}) \right] \tag{3}$$

UP_{LM} represents an upscaled pixel located at row L, column M, in the resultant upscaled image U_I. O_{ij} is the DN (digital number) of the pixel located in the original image at row i, column j, that is evaluated within the upscaled kernel. UP_{LM} and the pixels within rows ($i-k$, $j+k$) and columns ($i+k$, $j-k$) represent the same real-world extent. Thus U_I is composed of fewer pixels than O_I, though both represent the same geographic area. Resampling within the upscaling kernel is represented by the double summation of all DNs to a single object-weighted pixel value that is located within the new upscaled image. The non-overlapping kernel is then moved a distance of K pixels across O_I, and the process is iterated until a new upscaled image U_I is generated.

A multiscale extension: Iterative OSA and OSU

Although a single remote sensing scene represents a unique instance of all discernible objects within its extent, we hypothesize that it also contains additional information related to image-objects (IOs) that exist

over a 'limited' range of coarser, non-immediately discernible spatial scales, located within the same extent. Support for this comes from three sources:

1. Appreciating that both H- and L-res information exists within an image collected at a single resolution (Woodcock and Strahler 1987)
2. Understanding the intimate relationship between IFOV and object size (Slater 1980)
3. Recognizing that previous work illustrates the ability of OSU methods to reveal patterns that consistently model the spatial extent of differently sized objects existing at coarser scales (i.e., tree crowns, canopy gaps, etc, Hay et al. 1997).

To exploit this range of multiscale information within a single image, we hypothesize that by iteratively applying OSA to define object-specific (maximum and minimum) variance-thresholds within M_I, dominant landscape objects will emerge through the iteration process. In essence we are applying principles of non-linear feedback to ascertain if *self-organization* (Kay and Schneider 1995) – in the form of patterns corresponding to the spatial extent of dominant landscape objects – will 'emerge' at each new scale. We note that our goal in developing and applying object-specific techniques is to allow for *previously existing* self-organized patterns (i.e., image-objects) to be detected within the image/landscape at different scales. It is not to generate *new* self-organizing patterns. This subtle difference is important to clarify, because a strict requirement of self-organization includes temporal evolution (Nicolis and Prigogine 1989; Coveney and Highfield 1991), while a single remote sensing image – and all analysis performed on it – can only represent an instance in time.

The result of this iterative approach is a nested hierarchy of image-sets (IS_t) composed of V_I, A_I and M_I that have membership ($\in$) in a unique *scale domain* (SD_n). Within this SD_n, each image has the same grain and extent, and represents the results of multiscale analysis specific to the individual image-objects composing it. Following this logic, each SD_n is a member of a scale-domain super set (SDS) that represents the entire range of object-specific multiscale analysis (OSA) and scaling results (OSU) evaluated within the fixed spatial extent of a unique digital landscape (O_I). This hierarchical structure (outlined in Figure 6) may be described in the following manner:

$$P_{ij} \in IO_s \in IS_t \in SD_n \in SDS \quad (4)$$

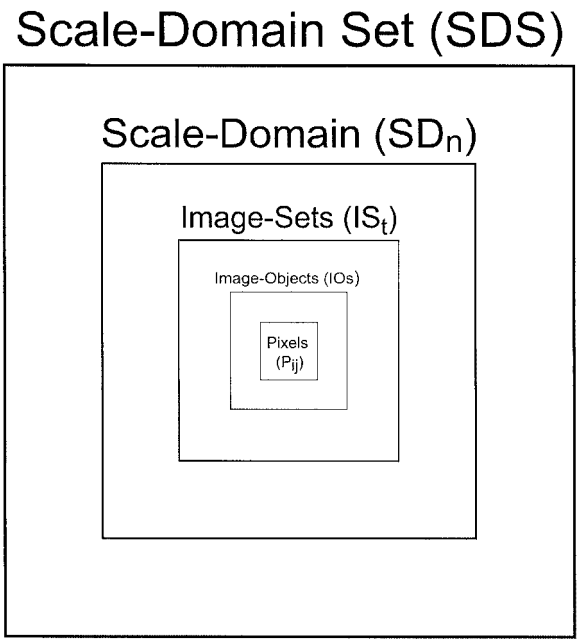

Figure 6. Hierarchically nested components of iterative object-specific analysis (OSA) and object-specific upscaling (OSU).

A digital landscape is composed of pixels (P_{ij}) that are parts of image-objects (IO_s), that are defined within a specific image-set (IS_t), that is a member of a scale-domain (SD_n), which populates a scale-domain set (SDS).

To operationalize this framework with minimal user-bias, we apply object-specific concepts to select the most appropriate images for upscaling. To minimize the *scale problem* resulting from arbitrary scaling, we apply a resampling heuristic (R_h) based on the relationship between image-objects and pixel size, and apply OSU as our upscaling algorithm (Hay et al. 1997). This combination of iterative OSA and OSU constitutes an *object-specific multiscale framework for landscape analysis* that is further discussed in the following sections.

Selecting an iterated M_I *to upscale*

Through the iteration process, M_I pixels increasingly become parts of objects existing over larger and larger extents, yet the spatial resolution of the pixels representing each new image-object remains constant. To reduce unnecessary computation, an appropriate M_I must be evaluated within each IS_t to determine if upscaling is necessary. In the first OSA iteration, the exact process described in section 'OSA and user-defined OSU' is applied. That is, each P_{ij} is assessed

within larger windows until a local *maximum* variance threshold ($VT_{w(max)}$) is reached that corresponds to a 'peak' location as illustrated by (A) in Figure 5. When applied to the entire image, this process generates the first image-set (i.e., V_1, A_1, M_1).

In the second iteration, each P_{ij} (in the newly generated M_1) is assessed within larger windows until a local *minimum* variance threshold ($VT_{w(min)}$) is reached. This results in the generation of a second image-set (i.e., V_2, A_2, M_2) that represents the beginning scales of all newly emergent image-objects. Conceptually, each pixel in M_2 will be represented by a local variance saddle or pit, as illustrated by (B) in Figure 5. Therefore, odd-numbered OSA iterations define scales representing the 'end' of objects, while even-numbered OSA iterations define the beginning scale of the next emergent object(s). As a result, all M_I generated from even-numbered OSA iterations will be selected for upscaling.

Defining an upscale resolution (R_h)

Once an appropriate image has been selected for scaling, the upscale resolution will be defined by a resampling heuristic (R_h) that is based on the relationship between pixel size, and the size of the minimum discernible image-object for which VT_w was initially developed. R_h is similar to recommendations by O'Neill et al. (1996), who suggest a grain size 2 to 5 times smaller than the spatial features of interest, and a sample area 2 to 5 times larger than the patches assessed. We note that this grain size recommendation corresponds to a reference by Slater (1980) regarding the point-spread function (PSF)[3] of the sensor. Essentially, if an object is less than $\frac{1}{4}$ the size of the sensor's IFOV, its influence in the corresponding pixel is equal to the sensor PSF. In modern sensors this value is exceptionally small, though it can be defined for each sensor, and included within the model. For the purpose of this study, R_h equals the resampling resolution where the minimum area (A_{min}) of all pixels composing the image-objects defined in A_I must be four times larger than the spatial resolution of the current image. This ensures not only detection (as implied by the $\frac{1}{4}$ PSF rule), but also identification (Jensen 1986). By adopting this 4:1 relationship we are again erring on the side of caution (i.e., under-sampling).

[3]The PSF defines the spatial influence or 'spread' of a zero-dimensional point of light resulting from lens aberrations in the sensor.

We also note, that if $\frac{1}{4}$ represents detection, and 4:1 represents identification, then a fuzzy (i.e., not specifically defined) range of scales (a maximum of) 16 times an object's minimum detectable size exists, where part of an object's spatial influence is potentially discernible within a single image. This further supports the hypothesis in the above section regarding a limited range of object-specific spatial information within a single image.

Upscaling strategy

In a previous study, Hay et al. (1997) evaluated OSU against four resampling or *scaling* techniques traditionally included in remote sensing image-analysis software. Over a gigabyte of data were analyzed and upscaled from 1.5 m to 3 m, 5 m, and 10 m, respectively, using nearest neighbor, bilinear interpolation, cubic convolution, non-overlapping averaging, and OSU. All upscaled images were evaluated against (non-upscaled) data of the same scene originally collected at a 10-m spatial resolution. The technique producing an upscaled image most visually and statistically similar to the original 10-m image was considered the most appropriate upscaling technique. Six thousand samples representing six different forest classes were evaluated using the smallest root-mean-square-error (RMSE) results to represent the best technique. Results indicate that OSU produced the most visually and statistically accurate upscaled images of those tested, with the lowest RMSE in 10 out of 18 classes over all forest types and ranges of scale tested. In the eight times it did not obtain the lowest RMSE, it produced six values with the second lowest errors. Based upon these results OSU is considered the most appropriate upscaling technique, thus it is used to resample the selected M_I to a resolution specified by R_h. To accomplish this, R_h is applied to Equation 1, replacing the user-defined upscaling kernel size (K). This iterative OSA and OSU strategy is then applied until VT_w is larger than the image dimensions.

Results

The original CASI image (O_I) spatially represents a complex forest scene spanning a geographic extent of 600 × 600 m. Spectrally it represents both the

Table 2. Image information and object-specific procedures for generating Figure 7.

SD_n	IS_t Components	OSA_t	OSU_n	M_I Dimensions	Grain (m^2)	# Pixels
SD_0	O_I		0	400×400	1.5	160000
	$IS_1 = V_1, A_1, M_1$	1		400×400	1.5	160000
	$IS_2 = V_2, A_2, M_2$	2		400×400	1.5	160000
SD_1	U_1		1	250×250	2.4	62500
	$IS_3 = V_3, A_3, M_3$	3		250×250	2.4	62500
	$IS_4 = V_4, A_4, M_4$	4		250×250	2.4	62500
SD_2	U_2		2	156×156	3.84	24336
	$IS_5 = V_5, A_5, M_5$	5		156×156	3.84	24336
	$IS_6 = V_6, A_6, M_6$	6		156×156	3.84	24336
SD_3	U_3		3	98×98	6.14	9604
	$IS_7 = V_7, A_7, M_7$	7		98×98	6.14	9604
	$IS_8 = V_8, A_8, M_8$	8		98×98	6.14	9604
SD_4	U_4		4	61×61	9.83	3721
	$IS_9 = V_9, A_9, M_9$	9		61×61	9.83	3721
	$IS_{10} = V_{10}, A_{10}, M_{10}$	10		61×61	9.83	3721

Table 3. List of Object-Specific terms and abbreviations.

$\forall$	For each. . .
$\in$	Has membership in. . .
$VT_{w(max)}$	Local *maximum* variance defined with the variance threshold window
A_I, A_{ij}, A_2	Area-image, Area value defined at (i, j), Area-image generated at OSA_2
EOs	Edge-objects
IOs	Image-objects
IS_t	Image-set generated at OSA iteration (t)
K, S_K	Upscaling kernel of (k^*k) user-defined dimensions, Sum of all A_{ij} within K
LTD_v	The Landscape-threshold-domain, where (v) represents the number of landscape thresholds defined by TSV within the SDS
M_I, M_{ij}, M_2	Mean-image, Mean value defined at (i, j), Mean-image generated at OSA_2
O_I	Original CASI image
OSA_t	Object-specific analysis at iteration (t)
OSU_n	Object-specific upscaling at the (n^{th}) upscaling iteration
P_{ij}	Pixel located at row (i), column (j) in a 2D image
R_h	Resampling heuristic
SD_n	Scale-domain, resulting from the (n^{th}) OSU iteration
SDS	Scale-domain-set
TSV	Total scene variance
U_I, U_2	Upscale-image, Upscale-image generated at OSA_2
UP_{LM}	An upscaled pixel located at row L, column M, in the U_I
V_I, V_{ij}, V_2	Variance-image, Variance value defined at (i, j), Variance-image generated at OSA_2
$VT_{w(max)}$	Local maximum variance defined with the variance threshold window
$VT_{w(min)}$	Local minimum variance defined with the variance threshold window
VT_w, VT_{ij}	Variance threshold window, Pixel location (i, j) defined at the variance threshold
W_{ijK}	Object-specific weight defined at row (i), column (j) within K

minimum chlorophyll *a* reflectance signal[4], and the absorption maximum of solvated chlorophyll a (Kirk et al. 1978). In this study, it is also considered a surrogate measure of vegetative 'greenness'. When the multiscale extension is applied to O_I, the result is a hierarchy of image-sets (SD_n), each consisting of variance (V_I), area (A_I), and mean images (M_I), with the same spatial resolution. As upscaling occurs, the spatial resolution of the newly generated image-sets increase as do their scale domain subscripts i.e., SD_{n+1}. The iteration where OSU first takes place is referred to as SD_1. The image-set prior to this is SD_0 - as upscaling is not applied. Figure 7 illustrates image-sets within the first four scale-domains (SD_{0-3}), generated from automatically applying 10 iterations of OSA, and 4 iterations of OSU to the original CASI image. The procedures for producing these results are outlined in Table 2, and are summarized as follows.

OSA was applied to the O_I where object-specific measures of maximum local variance were assessed for every pixel resulting in the first image-set (V_1, A_1, and M_1). OSA was then applied to the newly generated M_1, where object-specific measures of minimum local variance were similarly assessed, resulting in the second image-set (V_2, A_2, and M_2). Together, these image-sets and O_I represent the first scale domain (SD_0), of which V_2, A_2, and M_2 are illustrated in Figure 7. Based on the concepts described above, M_2 was automatically selected for upscaling to a resolution defined by R_h. This resulted in a grain change from 1.5 m to 2.4 m and the generation of the first upscaled image (U_1). These procedures were then repeated for the next 8 iterations, substituting in the appropriately defined M_I, R_h, and U_I variables. In all cases, the resulting upscale images (U_{2-4}) were used as the 'seed' images for OSA, from which new image-sets (IS_{3-10}) composing the additional scale-domains (SD_{1-4}) were generated. To facilitate visual comparisons[5] between the image-sets illustrated in Figure 7, each upscaled image was resampled to 400×400 pixels. Resampling was performed using nearest neighbor so that original DN values were not changed. As a result, images in latter scale-domains appear more 'blocky' than those in SD_0.

[4]Though radiometrically 'close', the low trough in spectra associated with plants is nearer to 675 nm than to the spectral band location (655–665 nm) defined in this data set.

[5]All figures are 8 bit linearly scaled versions of 16 bit data that have been enhanced for illustration. In the original images, far greater visual clarity is achieved than in print.

As the grain size increased through the upscaling process from 1.5 m to 9.83 m, the total number of pixels in the image was reduced from 160,000, to 3,721. Object-specific analysis was stopped at OSA_{10}, as analyzing kernels contacted the borders of the image. Throughout the scaling process, the scene extent remained constant at 600×600 m, but the physical dimensions of the generated images were systematically reduced from 400×400, to 61×61 pixels. The visual differences in information content resulting from these procedures are illustrated in Figure 8, where U_{1-4} is illustrated against the background of O_I. We note that OSU was applied to $M_{2,4,6,8}$ to generate this upscale composite.

Within each SD_n, the V_I represents a threshold-image resulting from OSA. Essentially it illustrates where the edges of differently sized objects have been reached. Bright tones define areas of high variance (object edges), while darker tones define areas of low variance (object interiors) e.g. bright road edges *vs.* dark young forest (image bottom) in V_2. Similarly, each A_I models the maximum spatial extent – or *area of influence* – of its constituent objects at a specific grain defined within the variance threshold kernel. This important measure represents the unique (scale-specific) areas over which dominant landscape objects exist, thus it is used to determine object-specific-weights for scaling. Because image-objects are composed of similar pixels, they tend to be assessed within smaller kernels, as their accompanying variance measures are small. This results in correspondingly small area values, which are visually represented by dark areas. In A_2, dark tones within the mature stand (image center) clearly correspond to individual tree crowns, while the brighter surrounding values correspond to edges composed of shadow and or understory pixels. Visually, these results strongly support the validity of objects-specific heuristics (at least over fine scales), as individual trees illicit complex illumination/shade effects on either side of their crown, yet both sides are considered part of a single object (i.e., a dark tone).

In each M_I every pixel represents a H-res member of a newly detected image-object that exists at its next (coarser) scale i.e., branches and leaves now become part of a tree crown. Because these images are generated from average values calculated within specific threshold kernels, they represent the dominant image structure defined at a specific spatial resolution within a unique scale-domain. To enhance interpretation of the overall structural evolution of each M_I composing SD_{1-4}, we have applied a simple linear color table, as

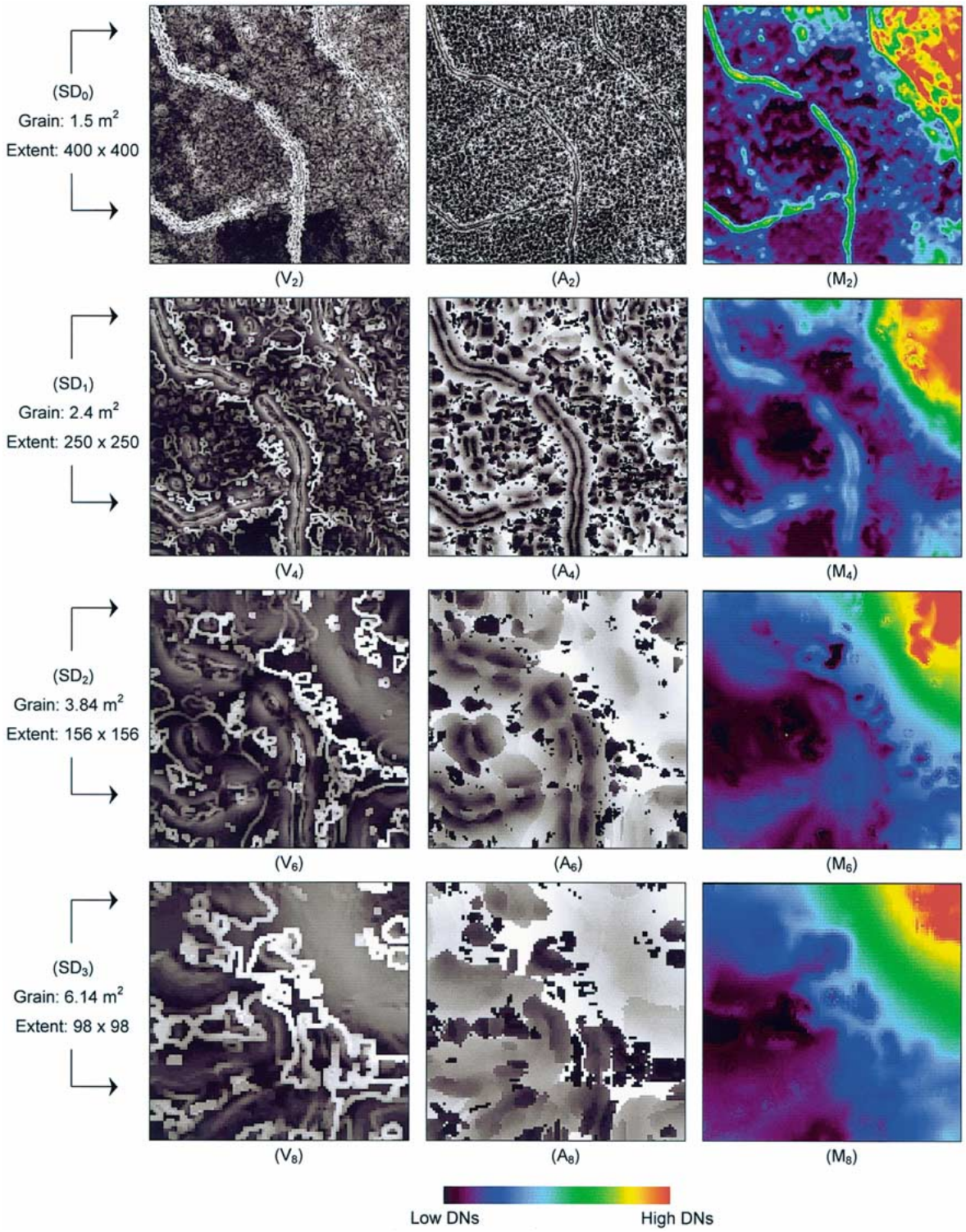

Figure 7. Scale domain sets (SDS_{0-3}) consisting of variance (V_I), area (A_I), and mean (M_I) images.

printed gray-tone gradations are more difficult to distinguish. In each M_I, black and purple represent high-density vegetation, dark blue represents low-density vegetation, and light blue-green represents the gradient between sparsely vegetated and non-vegetated areas. Clear-cut areas with varying amounts of vegetation range from green-yellow, where colors represent low-density invading grasses and shrubs on partially exposed soils, to orange-red, representing the maximum scene brightness resulting from fully exposed soils.

As the spatial resolution of each SD_n changes, each V_I, A_I, and M_I visually delineate newly defined scale-specific structures that represent the dominant objects emergent at these scales. In SD_0 a large amount of recognizable object structure is explicitly defined. In particular, individual tree crowns, their shadows, canopy gaps, patches of exposed soil and vegetation, road edges, and vegetation along roads are highly discernible in both V_2 and A_2. In SD_1 we see an obvious evolution from individual crown structures within the mature stand (as defined in V_2 and A_2), to larger sized objects (dark patches) that correspond to areas of high stand densities and include reflective characteristics from crowns, shadows, and understory. At this scale, the (highly reflective central) gravel road is influenced by the spectral characteristics of the surrounding vegetation, causing it to change from green-yellow (as depicted in M_2) to a light blue (in M_4). It is also important to note the increasing spatial effect (i.e., larger areas of bright tones in A_4) appearing along the edge of vegetated and non-vegetated areas. In V_4, this is represented by bright linear features around (darker) objects, and will be referred to further in the Discussion section.

In SD_{2-3} we see a dramatic change in the overall scene composition from the previous scale-domain sets. Here, the images clearly illustrate a distinct evolution within three dominant object groups: C.Cut (including roads, grasses, and bare soil depicted), young-forest (which includes young and juvenile classes), and mature forest. The net result is an increasing spatial and spectral encroachment of clear-cut, and low vegetation density areas within locations that were initially densely vegetated. This is most apparent in the upper right quadrant of each image, where the spatial influence of C.Cut, and lower density vegetation (i.e., young forest) increase at the expense of mature forest.

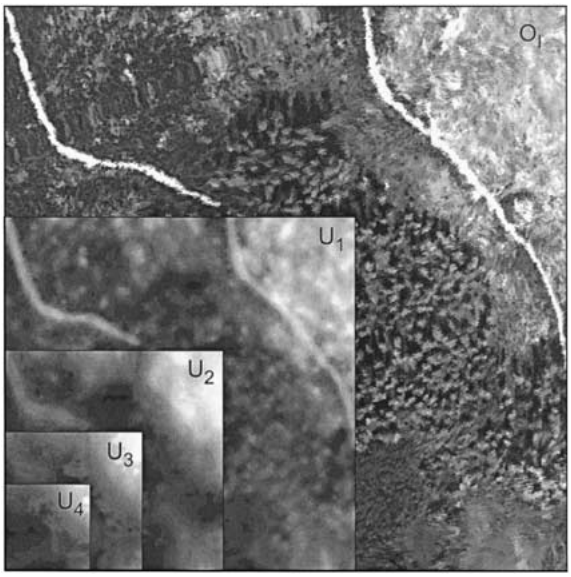

Figure 8. This upscale image (U_{1-4}) composite illustrates the different image extents resulting from four iterations of object-specific upscaling (OSU).

Discussion

What exists between the end of one image-object and the beginning of another?

We suggest that multiscale *image-object* thresholds are often far more 'fuzzy' or less discrete than the term *threshold* commonly implies. This is because the pixels used to evaluate image-thresholds are themselves a hemispherical integration of reflected light, which represents the non-linear interaction of entities existing over different scales. For example, a single 'threshold' pixel defining the extent of a tree-crown may share its composition with a portion of this crown's edge, the neighboring crown shadow, understory, and partial reflectance from near-by exposed soil. Therefore, rather than a pixel being part of a nested hierarchy of discrete image-objects that spatially lie adjacent to each other through scale, there exists instead, a unique range of scales between the end of one image-object, and the beginning of another, that is composed of integrated 'edge' pixels. We refer to the species of objects that populate this 'edge-space' as *edge-objects* (EOs), and suggest that an example of their signal is illustrated in Figure 5, between A–B, C–D, and E–F.

Conceptually, EOs exist within a varying range of scales located on the 'other-side' of discrete image-object frontiers or boundaries, but due to their digital

nature[6] they actually share part of their spectral composition with a non-linear integrated fraction of the edge pixels they abut. As a consequence, EOs will always be L-res which means they will be represented by relatively large V_I and A_I measures, as they are unable to be defined within the range of scales commonly used to assess image-objects (see Figure 7). For example, during OSA_1, visual and statistical output generated at each increment in window size indicated that 99% of O_I was processed within a window size of 29×29. Yet the remaining 1% required analysis up to a window size of 63×63. In addition, this 1% of pixels did not visually correspond to spatially meaningful image-objects within O_I. Instead, they represented edge locations between recognizable IOs. A similar trend was found in all additional iterations throughout the OSA process.

To ensure that spatially dominant image-objects will emerge through multiscale analysis, rather than EOs, we confirm that inverse area values (which favor image-objects) are used to define all OSU weights. And yet, EOs appear to spatially dominate at coarser grain sizes, rather than recognizable image-objects (see Figure 7). We suggest two plausible solutions for this condition. Either EOs represent real landscape structure(s), or they are artifacts resulting from inappropriate OSA heuristics.

Strong support that OSA heuristics work well on recognizable image-objects is provided by SD_0 in Figure 7, where individual tree crowns, road edges, canopy gaps, and barren areas have been explicitly delineated. When these results are considered in relation to the evaluation conducted during heuristic development, we are confident that the heuristics work well. The second solution is that EOs are actually image-objects that represent real multiscale landscape structure that we may not be familiar with from a single-scale perspective.

If edge-objects (EOs) are real, what landscape phenomenon do they model?

As Wu and Qi (2000) point out, it is not always clear whether the effect of changing scale is an artifact due to the improper use of analytical methods, an indication of the scale multiplicity of ecological systems, or neither of the two. If for a moment we consider that EOs are real landscape entities rather than image artifacts, what do they structurally represent? By their very nature, we know that they are not image-objects with obvious real-world counterparts, if they were, we would recognize them. Obviously we need to evaluate EOs with a different conceptual perspective. What we do know is that EOs exist in the 'edge-space' between image-objects. Visual analysis of Figure 7 reveals a spatial evolution of increasing perimeter for C.Cut, gravel-road, and barren-ground, that extends far beyond their initial physical boundaries (see Figure 4a). When these changes are considered in relation to the scale-dependent manner in which OSA functions, it is highly plausible that the evolution of EOs models the scale-dependent change(s) occurring at, or within, *ecotones*.

Although the study of ecotones is complicated by the diversity of interpretation regarding their nature, we adopt the definition of Holland (1988), where the transition zone between adjacent patches is recognized as an ecotone. In OSA, image-objects correspond to scale-dependent patches within a landscape mosaic, thus EOs correspond to their ecotones. A serious challenge with ecotone detection is the subjectivity inherent with identifying boundaries along gradually changing ecolines. Here the difficulty involves dividing a zone of 'continuous' variation into compartments. As Johnson et al. (1992) indicate, even when statistically significant differences exist between individual compartments, the boundaries between them may not represent true ecotones. Instead, ecotones span the range between these two extremes. In addition, boundary distinctness is scale dependent, thus users are also faced with the subjectivity of determining the most appropriate scale to assess the scene, which in turn effects the delineation of ecotones.

One of the true benefits of imaging spectrometry is the ability to explicitly link specific spectral characteristics with physiological properties (Wessman et al. 1989). If the idea of EOs as ecotones is linked with the spectral characteristics of the original CASI image (i.e., a surrogate measure of vegetative 'greenness') it is further plausible to hypothesize that EOs defined in O_I may be a visual analogue of what is referred to as '*depth-of-edge influence*', or '*edge width*' (Chen 1999). Depth-of-edge influence is associated with microclimatic zones across abrupt edges in the landscape, and can result in broad areas of edge influence, which constitute a significant portion of (unaccounted) fragmentation in a landscape. The phenomenon varies over time and with edge charac-

[6]Within a digital scene, an image-edge or threshold is not a 1D-line composed of zero-dimensional points lying between two or more pixels, but rather a 3D pixel (i.e., x, y, DN) that must exist in the same location as one of the points it is trying to segregate.

teristics, and can extend four to six tree heights into the forest from a recent clear-cut edge. Notably, edge-width value varies according to different tree species, ranging from 60 m in Eastern Red Pine/White Pine to over 400 m in Pacific N.W. Douglas-fir forests (Chen 1999). This 'EO = edge-width' hypothesis is further supported by the fact that O_I is a high-resolution scene of a (then) recently clear-cut site on southern Vancouver Island, where the dominant tree species in all three-forest classes (Mature, Young and Juvenile) are Pacific N.W. (Coastal) Douglas Fir. However, it is important to note that no microclimate data were available to corroborate this hypothesis. Nevertheless, this provides an excellent example of how object-specific analysis offers new insight into linking and questioning the relationships between landscape processes and multiscale landscape patterns, that may not have been possible without such a multiscale perspective.

Can an OSA perspective be used to define landscape-scale thresholds?

Through the iterative OSA and OSU process, the patterns generated within a SDS represent an evolution of image-objects from small-scale entities such as individual tree-crowns, to larger 'landscape' sized objects that will eventually dominate the entire image. From the results in Figure 7 it is clear that between SD_1 and SD_2, recognizable image-objects stopped being generated, and unfamiliar EOs began to emerge and dominate the scene. We suggest that this change in spatial dominance, from image-objects to EOs, corresponds to crossing a landscape-scale threshold, and that it can be defined in a similar fashion as individual image-object thresholds.

Recall that when applying OSA to detect object-specific thresholds, each pixel is evaluated as part of an individual image-object. Therefore, to detect a landscape-scale threshold within an OSA framework, all image-objects and EOs within a scene are evaluated as being part of a larger scene-object (i.e., a landscape-scale threshold-object) that spatially dominates the entire image/landscape being assessed. This is operationalized by evaluating the total scene variance (TSV) for each image in a nested hierarchy, where each image represents the same study area, but at a different grain size. The resulting signal is then plotted, and modeled revealing distinct saddles and peaks, which correspond to the beginning and end scales of landscape-scale threshold-objects. Essentially this is *scale variance analysis* as described earlier, except that within an OSA framework, the nested hierarchy corresponds to image-sets generated at each OSA iteration, and images representing different grain sizes are generated only at odd-numbered iterations (except for OSA_1). In addition, TSV is defined for each variance-image rather than each mean-image as object-specific structures are explicitly defined in V_I, while in M_I such structures are smoothed. In simple terms, these procedures correspond to evaluating the total difference in the variation resulting from the individual image-objects composing a scene through all possible object-specific scales of analysis.

To better understand the total scene variance and corresponding scene/landscape structure through scale, TSV values generated for each VI at odd numbered iterations[7] are modeled with a high order polynomial ($R^2 = 0.999$), and the resulting curve [Poly. (TSV)] is illustrated in Figure 9. We note that while the shape of this cure is similar to that found in Figure 5, it must be assessed with caution past iteration 8, as OSA_{8-10} kernels required analysis over larger window sizes than the available image dimensions. This indicates that the pixels being assessed were part of a larger-scale image-object that existed beyond the extent defined by the image. Visual analysis of Poly. (TSV) reveals a saddle at iteration 3 and a peak at iteration 6 indicating the beginning and end range of the first landscape-scale threshold-object. It is also possible that another landscape scale threshold begins at or after OSA_{11}. Recall from Table 2, that OSA_{3-4} are members of SD_1. When compared with the results in Figure 7, the first landscape-sized threshold corresponds explicitly to the visual changes between SD_1 and SD_2, supporting the idea that OSA can be used to evaluate a full-range of landscape thresholds ranging from small-scale image-objects to large-scale landscape structures.

Conclusion

From a multiscale perspective a scale-domain set may be visualized as a hierarchical scaling ladder (Wu 1999), and each SD_n may be visualized as an individual rung, separated by unequal spaces that are specific to the range of scales assessed within the ISt that composes it. Alternatively, since Figure 9 supports the detection of landscape-thresholds between

[7] We note that values generated at even-numbered iterations produced a very similar curve, transposed by one iteration in the x-axis.

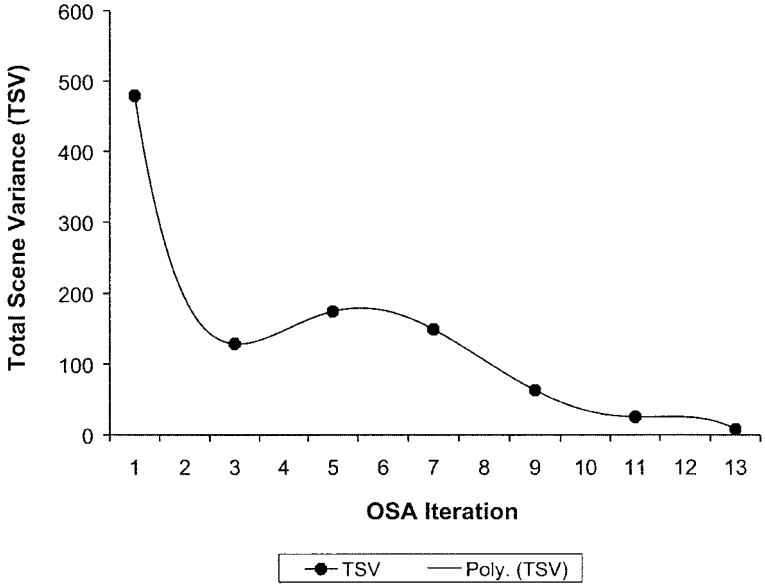

Figure 9. Total Scene Variance (TSV) defined at odd-numbered object-specific analysis (OSA) iterations. Poly.(TSV) represents TSV values modeled by a high order polynomial curve ($R^2 = 0.999$) that is similar to the curve illustrated in Figure 5.

adjacent SD_n, it may be more reasonable to include SD_n as a subset of a higher-order set we refer to as a *landscape-threshold-domain* (LTD_v), where the subscript (v) represents the number of different landscape thresholds defined by TSV within the SDS. Thus equation 4 should be augmented as follows:

$$P_{ij} \in IO_s \in IS_t \in SD_n \in LTD_v \in SDS \qquad (5)$$

As a result, it may be more appropriate to consider the landscape represented by a linked group of different sized scaling ladders, where each ladder corresponds to a specific LTD^v, rather than a single hierarchical scaling ladder as Wu (1999) suggests. Though originating from different starting points, we suggest that a multiscale OSA and OSU approach provides a methodological framework that is complimentary to the described theory, and techniques required by the Hierarchical Patch Dynamics Paradigm (HPDP) (Wu and Loucks 1995). HPDP provides a link between the patch dynamic perspectives and hierarchy theory that emphasizes multiscale properties of pattern and process dynamics in ecological systems. In this paradigm, individual patches are considered the fundamental structural and functional units. In OSA these primitives correspond to image-objects, whose spatial dimensions and influence can be defined and aggregated to unique coarser scales (i.e., OSU), specified by the dominant entities (A_I) composing a scene.

If at multiple image scales, the spatial extent of dominant A_I patterns strongly corresponds to geographic areas over which known processes are dominant (i.e., soils, slope, aspect), these areas may be selected as locations over which scale-dependent ecological models could be developed, or data explicitly translated to and from (Holling 1992). King (1990) identifies four general methods of translating ecological models to larger scales: (1) lumping, (2) direct extrapolation, (3) extrapolation by expected value, and (4) explicit integration. In particular, direct extrapolation could benefit from OSA because it involves explicitly running a small-scale model for a set of discrete elements, scaling the output of each element by the area represented, then combining the outputs to represent the large-scale system.

If we consider that the OSA and OSU heuristics are sufficiently robust, and that MAUP effects are minimized – through adopting an entity, or object-specific approach – then the complex patterns forming at each OSA iteration represent the emergence of real world structures existing, or imbedded at different scales within a single scale of imagery. Good reason exists to consider this a sound supposition, as (V_I) and (A_I) strongly correspond to real world scene-components, thus the heuristics defining image-object thresholds are being met. As threshold patterns emerge at each iteration, and their specific resolutions and extents are defined, the ideal situation would be for remote sens-

ing data – representing surrogate ecological measures [such as leaf area index (LAI), or fraction of photosynthetically active radiation, (FPAR)] – to be scaled with OSU and used as inputs into unique ecological models operating over the spatial extents defined by the corresponding A_I (Freidl 1997). Alternatively, model development and data type selection could be guided by the OSA scale-domains and landscape threshold patterns generated. If iterated OSA and OSU results correspond to field data over a range of known scales, precedent exits upon which to assess OSA and OSU results at coarser unverifiable image scales. At present, object topology is not embedded within the analyzing routines, but it is envisioned in subsequent versions, which will provide multiscale image-object output for use in geographic information systems.

In this paper we introduce a multiscale framework for analysis and upscaling that when applied to remote sensing imagery reduces the effects of MAUP by incorporating an object-specific approach. By considering landscapes as hierarchical structures and adopting this multiscale framework, the patterns of landscape objects operating at, and over, unique spatial scales may be thematically and numerically quantified by their spatial dominance. While aware that the entities that emerge in a data set are scaled by virtue of the observation protocol and the filters applied to the data during analysis, we suggest that multiscale OSA and OSU offers a potentially powerful framework for improved understanding of scale-specific landscape patterns. In particular, multiscale OSA may assist in defining critical landscape thresholds, domains of scale, ecotone boundaries, and the grain and extent at which scale-dependent ecological models could be developed and applied.

This paper provides only a small sample of the potential of multiscale OSA tested over a relatively fine geographic area. The next step is to apply these ideas over a larger-extent fine-grained scene, where sufficient ancillary data exist so that results may be fully verified over numerous spatial scales. To facilitate this, analysis is presently underway in the complex agro-forested Haut-Saint-Laurent region of Quebec to examine how landscape fragmentation and connectedness change through scale, and what their implications are for landscape management (Bouchard and Domon 1997; Pan et al. 2000). Our primary objective will be to apply the described object-specific framework to H-res Ikonos satellite data (acquired in September, 2000) that represents an 11 km × 11 km scene, and evaluate the multiscale results against a database representing more than 15 consecutive years of intensive field studies and research.

Acknowledgements

This work has been supported by a Biology graduate scholarship of excellence from the University of Montréal and a GREFi Ph.D. Scholarship awarded to Mr Hay, by the Ministry of Natural Resources Canada through its Human Resources Planning and Training Program, and by a team grant awarded to Dr A. Bouchard and Dr D. Marceau from FCAR, Gouvernement du Québec. We also express appreciation to Forestry Canada for the CASI imagery, Dr Marie Josée-Fortin for her assistance with algorithm notation, and to three anonymous referees for their constructive comments.

References

Allen, T.F.H. and Hoekstra, T.W. 1991. Role of heterogeneity in scaling of ecological systems under analysis. *In* Ecological Studies 86: Ecological Heterogeneity. pp. 47–68. Edited by J. Kolasa and S.T.A. Pickett, Springer-Verlag.

Allen, T.F.H. and Starr, T.B. 1982. Hierarchy Perspective for Ecological Complexity. University of Chicago Press, Chicago, 310 pp.

Amrhein, C. and Reynolds, H. 1996. Using spatial statistics to assess aggregation effects. Geogr. Syst.3: 143–158.

Benson, B.J. and MacKenzie, M.D. 1995. Effects of sensor spatial resolution on landscape structure parameters, Landscape Ecol. 10: 113–120.

Bian, L. and Walsh, S.J. 1993. Scale dependencies of vegetation and topography in a mountainous environment of Montana, The Professional Geographer 45: 1–11.

Bouchard, A. and Domon, G. 1997. The transformation of the natural landscapes of the Haut-Saint-Laurent (Québec) and its implication on future resources management. Landscape Urban Plan. 37: 99–107.

Caldwell, M.M., Matson, P.A., Wessman, C. and Gamon, J. 1993. Prospects for scaling, in Scaling Physiological Processes: Leaf to Globe. pp. 223–230. Academic Press.

Chen. J, Saunders, S.C., Crow, T.R., Naiman, R.J. 1999. Microclimate in forest Ecosystems and Landscape Ecology. Bioscience 49: 288–297.

Coveney, P. and Highfield, R. 1991. The Arrow of Time. Flamingo Press, London, 378 pp.

Cullinan, V.I., Simmons, M.A. and Thomas, J.M. 1997. A bayesian test of hierarchy theory: scaling up variability in plant cover from field to remotely sensed data. Landscape Ecol. 12: 273–285.

Curran, P.J. and Atkinson, P.M. 1998. Geostatistics and Remote Sensing. Progr. Phys. Geogr. 22: 61–78.

DeFries, R.S., Townshend, J.R. and Los, S.O. 1997. Scaling land cover heterogeneity for global atmosphere-biosphere models. pp. 231–246. *In* Scale in Remote Sensing and GIS, Lewis Publishers.

Dudley, G. 1991. Scale, aggregation, and the modifiable areal unit problem. The Operational Geographer 9: 28–33.

Duggin, M.J. and Robinove, C.J. 1990. Assumptions implicit in remote sensing data acquisition and analysis. Int. J. Remote Sensing 11: 1669–1694.

Ehleringer, J.R and Field, C.B. (Eds), 1993. Scaling Physiological Processes: Leaf to Globe. Academic Press, 388 pp.

Fotheringham, A.S. 1989. Scale-independent spatial analysis. pp. 221–228. *In* Accuracy of Spatial Databases, Taylor and Francis.

Fotheringham, A.S. and Wong, D.W.S. 1991. The modifiable areal unit problem in multivariate statistical analysis. Environment and Planning A, 23: 1025–1044.

Freidl, M.A. 1997. Examining the Effects of Sensor Resolution and Sub-Pixel Heterogeneity on Spectral Vegetation Indices: Implications for Biophysical Modeling. pp. 113–139. *In* Scale in Remote Sensing and GIS, Lewis Publishers.

Friedl, M.A., Davis, F.W., Michaelsen, J. and Moritz, M.A. 1995. Scaling and uncertainty in the relationship between the NDVI and land surface biophysical variables: An analysis using a scene simulation model and data from FIFE. Remote Sensing of Environment 54: 233–246.

Gardner, R.H. 1998. Pattern, Process, and the Analysis of Spatial Scales. pp. 17–34. *In* Ecological Scale Theory and Applications. Columbia University Press.

Gardner, R.H., Cale, W.G. and O'Neill, R.V. 1982. Robust analysis of aggregation error. Ecology 63: 1771–1779.

Hay, G.J., Niemann, K.O. and Goodenough, D.G. 1997. Spatial thresholds, image-objects, and upscaling: A multiscale evaluation. Remote Sensing of Environment 62: 1–19.

Hay, G.J., Niemann, K.O. and McLean, G.F. 1996. An object-specific image-texture analysis of H-resolution forest imagery. Remote Sensing of Environment 55: 108–122.

Holland, M.M, 1988. SCOPE/MAP technical consultations on landscape boundaries. Biol. Intl. 17: 47–106.

Holling, C.S. 1992. Cross-scale morphology, geometry, and dynamics of ecosystems. Ecol. Monogr. 62: 447–502.

Hunt, L. and Boots, B. 1996. MAUP effects in the principal axis factoring technique, Geogr. Syst. 3: 101–121.

Jarvis, P.G. 1995. Scaling processes and problems. Plant Cell Environ. 18: 1079–1089.

Jelinski, D.E. and Wu, J. 1996. The modifiable areal unit problem and implications for landscape ecology. Landscape Ecol. 11: 29–140.

Jensen, J.R. 1986. Introductory Digital Image Processing, Prentice-Hall, Englewood Cliffs, NJ, 379 pp.

Johnston, C.A., Pastor, J. and Pinay, G. 1992. Quantitative Methods for studying Landscape Boundaries. *In* Landscape Boundaries. Consequences for Biotic Diversity and Ecological flows. pp. 107–125. Springer-Verlag.

Kay, J.J. and Schneider, E.D. 1995. Embracing Complexity: The Challenge of the Ecosystem Approach. pp. 49–59. *In* Perspectives on Ecological Integrity, Kluwer, Dordrecht.

King, A.W. 1999. Hierarchy Theory and the Landscape . . . Level? Or: Words do Matter. Issues in Landscape Ecology. pp. 6–9. Edited by J. Wiens, M. Moss. International Association for Landscape Ecology. Fifth World Congress. Snowmass Village, Colorado, USA.

King, A.W. 1990. Translating models across scales in the landscape. *In* Quantitative Methods in Landscape Ecology, pp. 479–517, Springer-Verlag.

Kirk, O. and Tilney-Basset, R.A.E. 1978. The Chlorophylls. The Plastids. Their Chemistry, structure, growth and inheritance. pp. 64–89. Freeman & Co. LTD.

Levin, S.A., 1992. The problem of pattern and scale in ecology. Ecology 73: 1943–1967.

Mandelbrot, B. 1967. The Fractal Geometry of Nature. Science 156: 636–642.

Marceau, D.J. 1999. The scale issue in the social and natural sciences. Can. J. Remote Sensing 25: 347–356.

Marceau, D.J. and Hay, G.J. 1999a. Contributions of remote sensing to the scale issues. Can. J. Remote Sensing 25: 357–366.

Marceau, D.J. and Hay, G.J. 1999b. Scaling and Modelling in Forestry: Applications in Remote Sensing and GIS. Can. J. Remote Sensing 25: 342–346.

Marceau, D.J., 1992. The problem of scale and spatial aggregation in remote sensing: An empirical investigation using forestry data. Unpublished Ph.D. thesis, Department of Geography, University of Waterloo, 180 pp.

Marceau, D.J., Howarth, P.J. and Gratton, D.J. 1994. Remote sensing and the measurement of geographical entities in a forested environment; Part 1: The scale and spatial aggregation problem. Remote Sensing Environ. 49: 93–104.

Meentemeyer, V. 1989. Geographical perspectives of space, time, and scale. Landscape Ecol. 3: 163–173.

Moellering, H. and Tobler, W. 1972. Geographical variances. Geogr. Analysis 4: 34–64.

Moody, A. and Woodcock, C.E. 1995. The influence of scale and the spatial characteristics of landscapes on land-cover mapping using remote sensing. Landscape Ecol. 10: 363–379.

Nicolis, G. and Prigogine, I. 1989. Exploring Complexity. W.H. Freeman, New York, 313 pp.

O'Neill, R.V. and King, A.W. 1998. Homage to St. Michael; Or, Why are there so many books on Scale? *In* Ecological Scale Theory and Applications. pp. 3–15. Columbia University Press.

O'Neill, R.V., De Angelis, D.L., Waide, J.B. and. Allen, T.F.H. 1986. A hierarchical concept of ecosystems. Princeton University Press, Princeton, New Jersey, 262 pp.

O'Neill, R.V., Hunsaker, C.T., Timmins, S.P., Jackson, B.L., Jones, K.B., Ritters, K.H. and Wickham, J.D. 1996. Scale problems in reporting landscape patterns at the regional scale, Landscape Ecol. 11: 169–180.

O'Neill, R.V., Johnson, A. R. and King, A.W. 1989. A hierarchical framework for the analysis of scale. Landscape Ecol. 3: 193–205.

Openshaw, S. 1981. The modifiable areal unit problem. *In* Quantitative Geography: A British View. pp. 60–69. Routledge and Kegan Paul, London.

Openshaw, S. 1984. The Modifiable Areal Unit Problem. Concepts and Techniques in Modern Geography (CATMOG) No. 38, 40 pp.

Openshaw, S. and Taylor, P. 1979. A million or so correlation coefficients: three experiments on the modifiable areal unit problem. *In* Statistical Applications in the Spatial Sciences. pp. 127–144. London Pion.

Pan, D., Domon, G., Marceau, D.J. and Bouchard, A. 2001. Spatial pattern of coniferous and deciduous forest patches in an Eastern North America agricultural landscape: The influence of land-use and physical attributes. Landscape Ecol. 16: 99–110.

Pax-Lenney, M. and Woodcock, C.E. 1997. The effect of spatial resolution on the ability to monitor the status of agricultural lands. Remote Sensing Environ. 61: 210–220.

Slater, P.N. 1980. Remote Sensing: Optics and Optical Systems. Addison-Wesley, 575 pp.

Souriau, M. 1994. Scaling and physical thresholds: The case of continental topography. Int. J. Remote Sensing 15: 2403–2408.

Stewart, J.B., Engman, E.T., Feddes, R.A. and Kerr, Y.H. 1998. Scaling up in hydrology using remote sensing: summary of a Workshop. Int. J. Remote Sensing 19: 181–194.

Townsend, P.A. 2000. A Quantitative Fuzzy Approach to Assess Mapped Vegetation Classifications for Ecological Applications. Remote Sensing of Environ. 72: 253–267.

Treitz, P. and Howarth. P. 2000. High Spatial Resolution Remote Sensing Data for Forest Ecosystem Classification: An Examination of Spatial Scale. Remote Sensing Environ. 72: 268–289.

Turner, S.J., O'Neill, R.V., Conley, W., Conley, M.R. and Humphries, H.C. 1991. Pattern and Scale: Statistics for Landscape Ecology. *In* Quantitative Methods in Landscape Ecology. pp. 19–49. Springer Verlag.

Ustin, S.L., Smith, M.O. and Adams, J.B. 1993. Remote sensing of ecological processes: A strategy for developing and testing ecological models using spectral mixture analysis. *In* Scaling Physiological Processes: Leaf to Globe. pp. 339–357. Academic Press.

Walsh, S.J., Moody, A., Allen, T.R. and Brown, D.G. 1997. Scale dependence of NDVI and its relationship to mountainous terrain. *In* Scale in Remote Sensing and GIS, Lewis Publishers pp. 27–55.

Wessman, C.A., Aber, J.D. and Peterson, D.L. 1989. An evaluation of imaging spectrometry for estimating forest canopy chemistry. Int. J. Remote Sensing 10: 1293–1316.

Wiens, J.A. 1989. Spatial scaling in ecology. Functional Ecol. 3: 385–397.

Woodcock, C.E. and Strahler, 1987. The factor of scale in remote sensing. Remote Sensing Environ. 21: 311–332.

Wu, J. 1999. Hierarchy and Scaling: Extrapolating Information Along A Scaling Ladder. Can. J. Remote Sensing 25: 367–380.

Wu, J. and Loucks, O.L. 1995. From balance of nature to hierarchical patch dynamics: a paradigm shift in ecology. Quater. Rev. Biol. 70: 439–466.

Wu, J. and Qi, Y. (in press). Dealing with scale in landscape analysis: An overview. Geogr. Inform. Sci., 6: 1–5.

Wu, J., Jelinski, D. E., Luck, M. and Tueller, P.T. (in press). Multiscale Analysis of Landscape Heterogeneity: Scale Variance and Pattern Metrics. Geogr. Inform. Sci., 6: 6–19.